

Vol. 22

No 1

2016



JOURNAL OF THE BALKAN TRIBOLOGICAL ASSOCIATION™[®]

Editorial Board

Honorary and Founding Editor

Prof. Dr. Nyagol Manolov, Bulgaria

Editor-in-Chief

Prof. Dr. Slavi Ivanov, Bulgaria

Editors

Assoc. Prof. Dr. Zh. Kalitchin, Bulgaria

Mag. Eng. M. Boneva, Bulgaria

Associate Editors

Prof. Dr. Nicolae Napoleon Antonescu,

Romania

Prof. Dr. Eng. habil. K.-D. Bouzakis,

Greece

Prof. Dr. Branko Ivković, Serbia

Prof. Dr. Mehmet Karamis, Turkey

Assoc. Prof. Dr. V. Gecevska,

FYR Macedonia

Assoc. Prof. Dr. Mara Kandeva,

Bulgaria

International Editorial Board

Prof. Dr. Vladimir Andonovic,

FYR Macedonia

Prof. Dr. Miroslav Babić, Serbia

Prof. Dr. G. Haidemenopoulos,

Greece

Prof. Dr. H. Kaleli, Turkey

Prof. Dr. A. Michailidis, Greece

Prof. Dr. Nikolai K. Myshkin, Belarus

Prof. Dr. S. Mitsi, Greece

Prof. Dr. P. St. Petkov, Bulgaria

Prof. Dr. Alexander Rač, Serbia

Prof. Dr. R. G. Ripeanu, Romania

Prof. Dr. Andrei Tudor, Romania

Prof. Dr. G. E. Zaikov, Russia

Assist. Prof. Dr. Afsin Alper Cerit,

Turkey

Assoc. Prof. Dr. Friedrich Franek,

Austria

Assoc. Prof. Dr. Mikolai Kuzinovski,

FYR Macedonia

Assoc. Prof. Dr. Fehmi Nair, Turkey

Assoc. Prof. Dr. V. Pozhidaeva,

Bulgaria

Assoc. Prof. Dr. Burhan Selcuk, Turkey

Scientific
Bulgarian
communications
Ltd., Co.

CONTENTS

Vol. 22, No 1, 2016

<i>Tribotechnics and tribomechanics</i> N. STOICA, A. TUDOR. Some Aspects Concerning the Thermoelastic Distortions of the Brake Drum-shoe Contact, with Application to Vehicles	1
<i>Tribotechnics and tribomechanics – prolongation of firearm lifetime</i> D. JOVANOVIĆ, B. STOJANOVIĆ, R. JANJIĆ. Capacity for Improving Tribological Characteristics of Barrel Interior Line on a Gun	17
<i>Tribotechnics and tribomechanics – tensile strength of steel-plastic geogrids</i> FAN PENG-FEI. Study on Tensile Property of the Steel-plastic Geogrid	28
<i>Tribotechnics and tribomechanics – measurement of resistance in elasto-hydrodynamic contacts</i> C. SACHANAS, A. MOISIADIS, A. MIHAILIDIS. Electrical Contact Resistance Measurement in Elasto-hydrodynamic Contacts	32
<i>Tribotechnics – dynamic oscillation features</i> G. POPA, C.-N. BADEA, A. BADEA, V. ŞTEFAN, E. C. BOJE, G. DUMITRU. Dynamic Oscillations Features of the Br 185 Locomotive Series	48
<i>Tribotechnics and tribomechanics – memory alloys</i> K. ALDAŞ, I. ÖZKUL. Determination of the Transformation Temperatures of Aged and Low Manganese Rated Cu-Al-Mn Shape Memory Alloys	56
<i>Tribotechnics – statistic energy analysis</i> XING PENG, HUA LIN, LÜ CHIHUA, DENG SONG, SU ZHUOYU. Analysis and Optimising Approach for Inner Noise Control Based on Statistical Energy Analysis	66
<i>Tribotechnics – tungsten welding of aluminium</i> S. AMAL BOSCO JUDE, G. R. JINU, P. ARUL FRANCO, MC. LURET. Microstructural Characterisation and Mechanical Properties on the Effect of Weld Speed in Autogenous TIG (Tungsten Inert Gas) Welded AA7075 Butt Joints	79
<i>Tribotechnics – smart electric vehicle</i> S. F. LIU, M. H. LEE. User-oriented Prospective Smart Electric Vehicles Innovating Design Development	93
<i>Technological tribology – working performance of pumping units</i> FENG ZI-MING, FANG XIN, DING HUAN-HUAN. Study on Working Performance of Phased Beam Pumping Unit	104
<i>Regulation of yaw phenomena</i> JIAN HU, LINWEI CAO, ZHANJIN WANG, GANGYAN LI. Automotive Yaw Rate Coordinated Control in Advance under Urgent Steering Condition Based on Active Front Steering and Differential Braking	112
<i>Computer simulations – molten steel flow, large eddy simulation</i> LI CHAO, BAI MINGHUA. Large Eddy Simulation (LES) of the Molten Steel Flow of Continuous Jumbo Billet Casting Mold Using $k-\epsilon$ Two-equation	130
<i>Computer simulations – social tribology</i> HUANG SHAO-BIN, LI YAN-MEI, LI YA, XU LI, SHEN LIN-SHAN. Research of a Kind of XML Matching Mechanism	142
<i>Tribotesting and electrical systems load forecasting</i> LIU QI, HUANG ZHENZHEN, LI SHENG. Research on Power Load Forecasting Based on Support Vector Machine	151
<i>Design and calculation of tribosystems</i> ZHONGJIU ZHENG. Optimum Global Sliding Mode Controller for DC Motor Servo System Based on Disturbance Observer	160
JIAN HU, WEI FAN, ZIRU NIU, GANGYAN LI. Digital Design Method of Variable Ratio Gear for Automobile Recirculating Ball Variable Ratio Steering Gear Based on Meshing Theory	171
JIAN HU, KAIKAI DONG, ZIRU NIU, GANGYAN LI. Digital Design Method of Variable Ratio Gear Pair for Automobile Mechanical Variable Ratio Steering Gear Based on Enveloping Simulation	184
CHUANXI LIU. Optimum Imaging Time Selection for ISAR Targets with Complex-motion	200
<i>Design and calculation of tribosystems – calibration of gear pumps</i> LIN HAI-BO, PAN WAN-GUI. A New Method for Calibrating Vision Measuring Systems Based on the Black-White Square Array and Its Application	210
<i>Vibration phenomena – acoustic emissions for recognition of coal rock stability</i> JING LI, JIANHUA YUE, YONG YANG, LI ZHAO. Acoustic Emissions Waveform Analysis for the Recognition of Coal Rock Stability	220
<i>Friction and wear of sintered materials in the presence of nanodiamonds</i> E. E. FELDSHTEIN, L. N. DYACHKOVA. The Use of Nanodiamonds to Improve Tribological Properties of Sintered Antifriction Materials	227
<i>Wear properties of aluminum alloy</i> M.OVUNDUR, F. MUHAFFEL, H. CIMENOGLU. Characterisation and Tribological Properties of Hard Anodised and Micro-arc Oxidised 5754 Quality Aluminum Alloy	233
<i>Wear and corrosion</i> R. G. RIPEANU, M. MINESCU, C. A. NITA. Wear Behaviour of Antifriction Coatings Applied at Parallel Gate Valves	240
<i>Wear – influence of molybdenum coating on fretting</i> D. BADOIU, G. TOMA. On a Dynamic Optimisation Problem of the Quadrilateral Mechanism	250
<i>Wear behaviour of stainless steel</i> E. NALCACIOGLU, D. OZYUREK, K. CETINKAYA. Investigation of the Effect of Molybdenum Amount on Wear Behaviour of 17-4 PH Stainless Steel Produced by Powder Metallurgy	261
<i>Wear – rating life of cylindrical roller bearings</i> S. CREŢU, M. BENCHEA, A. IOVAN-DRAGOMIR. On Basic Reference Rating Life of Cylindrical Roller Bearings. Part II. Elastic-Plastic Analysis	272
<i>Friction coefficient in gear pair</i> L. IVANOVIC, T. MACKIC, B. STOJANOVIC. Analysis of the Instantaneous Friction Coefficient of the Trochoidal Gear Pair	281
<i>Wear behaviour of deep cryogenic treated steel</i> K. AMINI, M. SAFARI, A. SHAFYEL. Investigation of Hardness and Wear Behaviour of the Deep Cryogenic Treated 1.3255 Tool Steel	294

see b.c.

<i>Wear resistance of coating surface layers</i>	
T. PETROV, P. TASHEV, M. KANDEVA. Wear Resistance of Surface Layers Modified with Al ₂ O ₃ and TiCN Nanopowders Weld Overlaid Using TIG and ITIG Methods.....	304
<i>Tribochemistry – special materials in military and space technologies</i>	
J. ALEXANDER, B. S. M. AUGUSTINE. Influence of Microwave Post Curing on the Mechanical and Thermal Properties of Basalt / Epoxy Composites for Aerospace Applications.....	316
<i>Coatings – friction in brake pads</i>	
B. GUNEY, I. MUTLU, A. GAYRETLI. Investigation of Braking Performance of NiCrBSi Coated Brake Discs by Thermal Spraying and Melting.....	331
<i>Coating tribology</i>	
S. MITROVIC, D. ADAMOVIĆ, F. ZIVIC, D. DZUNIC, M. PANTIC, D. JEVREMOVIC. Dry Sliding Wear Behaviour of PVD TiN Coatings for Cold Forming Tools.....	347
<i>Coatings – wear intensity measurements</i>	
J. NAPIORKOWSKI, P. SZCZYGLAK, K. LIGIER, R. KUCZYNSKI. Testing the Wear Intensity of Thin Coatings by the Ball-cratering Method in the Process of Selecting Punching Die Materials.....	356
<i>Coatings – chromium oxide films</i>	
ZHOU SIHUA, GUO YANHUA, ZHOU XIAODONG, LI JIN, TIAN CANXIN. Effect of Technical Parameters on Structure and Deposition Rate of Chromium Oxide Films Prepared by Magnetron Sputtering.....	363
<i>Special materials in mechanics and tribology</i>	
V. ERTURUN, S. KUMRU, H. FIDAN. Aging Effects on the Microstructure of a Tungsten Inert Gas Welded AA2024 Alloy.....	372
<i>Composite materials</i>	
KAN XINRONG, FENG XIAOXIN, ZHANG DONGMEI, SUN HUI, WANG XIAOYAN, YU XIAODONG, SUN HUZA. Study on the Alkali-activated Cementitious Materials Prepared with Alkali Slag.....	384
<i>Biotribology – ex-poro-hydrodynamic lubrication</i>	
M. RADU, T. CICONE. Experimental Determination of the Damping Capacity of Highly Compressible Porous Materials Imbibed with Water.....	390
<i>Biotribology – treatment with medicinal compounds of human joints</i>	
VL. BOYADZHEVA, N. STOILOV, R. STOILOV, G. PETROVA, S. STEFANOV, D. MEDJIDIEVA. Cost of Treatment of Rheumatoid Arthritis, Ankylosing Spondylitis and Psoriatic Arthritis with Biological Disease-modifying Antirheumatic Drugs in the Period 2013–2014 in Bulgaria.....	401
<i>Lubrication – effect of additives on friction coefficients</i>	
M. SIMSEK, O. NTEZIYAREMYE, E. DURAK. Additive Effects on Wear and Friction Performance of Micro-arc Oxidative Coated Journal Bearings.....	410
<i>Lubrication – computer simulation</i>	
D. MILOSEVIC, N. JANJIC, M. VULOVIC, Z. ADAMOVIĆ. Optimisation of Preventive Maintenance of Lubrication Subsystem by Reliability Simulation Model of V46-6 Engine.....	419
<i>Lubrication – effect of pseudo-plastic lubricants and surface roughness</i>	
J. JAVOROVA, K. STANULOV, A. ALEXANDROV, V. ILIUTA. Journal Bearings Lubrication of Non-Newtonian Lubricants with Surface Roughness Effects.....	433
<i>Role of tribology in sustainable development</i>	
WANG MIN, CHENG WEN, MIN LIANG, ZHENG JIAN-GANG, FANG YONG. Distribution and Correlation of Nutrients and Particle Size in Surface Sediments of Tang-pu Reservoir.....	444
<i>Polymeric materials – friction-related behaviour of polymer compounds used in the construction of coaxial sealing systems</i>	
A. DEACONESCU, T. DEACONESCU. Low Friction Materials Used in the Construction of Hydraulic Sealing Systems in the Case of Small Velocities.....	454
<i>Management and organisation of the production – land sliding and land slipping</i>	
LEI XU, DALI GUO, XIAOHUI ZENG, XIJUN KE. Productivity Simulation and Fracturing Treatment Parameters Optimisation for Oil Wells in Low Permeability Bottom Water Reservoirs.....	464
<i>Machinery breakdown – preventive maintenance</i>	
D. SPASIC, N. JEVTIC, Z. JANJIC, Z. ADAMOVIĆ. Electrohydraulic System for Automatic Gage Control (AGC) for Tandem Cold Mill Plant in Steelworks Smederevo.....	471
<i>Ecological tribology – risk assessment of hazardous gas transportation</i>	
ENRONG ZHANG, WENXUAN WANG, LING WU, PING LI. Research on the Diffusion of Hazardous Gas Leakage in Road Transportation and Its Influencing Factors.....	483
<i>Machinery breakdown – semantic survey-based risk management</i>	
WEN LU, SHIDONG FAN, JIYIN CAO. Research on Semantic Survey-based Ship Machinery Health Management Method Considering Ship Structure and Rule-based Document.....	493
<i>Tribology in construction engineering – effect of deformation in CFG pile</i>	
FEI HUA, D. TARTAKOVSKY, DAWEI SUN. Effect of Deformation of the CFG (Cement Fly-ash Gravel) Pile Group on the Adjacent Metro Tunnel Based on the Equivalent Material.....	507
<i>Contacts – adsorption isotherm</i>	
LIANG QIN, LI MIN. Study on Logging Interpretation for Shale Gas Reservoirs.....	516
<i>Information</i>	
The 2015 Tribology Gold Medal Awarded to Professor Shizhu Wen.....	522
New Member of the International Editorial Board – Assoc. Prof Dr. Friedrich Franek.....	523
New Member of the International Editorial Board – Prof. Dr. Nikolai K. Myshkin.....	524
Instruction to Authors.....	527

WEAR RESISTANCE OF SURFACE LAYERS MODIFIED WITH Al_2O_3 AND TiCN NANOPOWDERS WELD OVERLAID USING TIG AND ITIG METHODS

T. PETROV^a, P. TASHEV^b, M. KANDEVA^c

^a *Technical University of Sofia, Branch Plovdiv, Plovdiv, Bulgaria*

E-mail: petod@abv.bg

^b *Institute of Metal Science, Equipment and Technologies, Bulgarian Academy of Sciences, Sofia, Bulgaria*

E-mail: ptashev@ims.bas.bg

^c *Tribology Centre, Faculty of Industrial Engineering, Technical University of Sofia, Sofia, Bulgaria*

E-mail: kandevam@gmail.com

ABSTRACT

During the recent decade the processes and technologies based on energy heat sources are increasingly used for manufacture of new machine parts or restoration of worn ones. The surfaces with nanomodified overlaid layers exhibit increased hardness, wear resistance, corrosion resistance, etc. Moreover, satisfactory manufacture effectiveness is achieved because of the minimum allowances for mechanical processing. The processes of weld overlay also allow to control the chemical content and the phase content of the layers obtained.

This work suggests a new approach to the modification of surface layers with nanoparticles of carbide-, nitride-, oxide- and other powders. The addition of the particles is implemented within the low-temperature area of the weld pool, thus preventing their overheating. The structure and the microhardness of the surface layers modified with nanopowders of Al_2O_3 and TiCN and overlaid using Tungsten inert gas (TIG) and Impulse TIG (ITIG) methods are examined. Obtained are experimental data for the characteristics of wear and the wear resistance of coatings in conditions of dry abrasive friction.

Keywords: nanopowders, weld overlay, TIG weld overlay, ITIG weld overlay, wear resistance.

* For correspondence.

AIMS AND BACKGROUND

The addition of small quantities of highly heat-resistant nanopowders to traditional metallic alloys reveals new possibilities to improve their mechanical characteristics and to extend their areas of application.

A lot of studies discuss the influence of titanium-containing nanoparticles on the characteristics of the metal after weld overlay. In most cases, titanium carbonitride¹ or silicon carbide is used². It is found that the increase of the quantity of titanium-containing inclusions changes the microstructure of the metal and improves its mechanical properties, e.g. hardness and wear resistance. Beneficial results are achieved when nanomodifiers are added during the process of casting³ or weld overlay⁴⁻⁶. The increased hardness and considerable strength are probably due to the more fine-grain structure and the re-distribution of the inner stresses resulting from the nanopowders added. Usually, the powders used contain particles with dimensions of a few tens of nanometers⁷. The mechanical characteristics of the overlaid metal are maximally improved at medium concentration levels of nanoparticles⁸⁻¹², which is explained with the more fine-grain microstructure obtained.

The processes of powder weld overlay allow adjustment of both chemical and phase content of the overlaid layer¹³. The method for alloying of surface layers¹⁴ with carbide-, nitride-, oxide-, etc. powders size of nanosized particles can be also pointed as a new approach.

The composite¹⁴ materials obtained provide a new qualitative leap to increase the power of engines, energy- and transport plants, and to reduce of the mass of machinery and various devices¹⁵. The implemented TIG and ITIG methods for weld overlay are not highly-productive methods like the plasma powder weld overlay due to the lower power of the arc. However, these methods enable weld overlay on relatively small surfaces, such as blades, wear resistant plates, etc.



Fig. 1. Nanopowders of Al_2O_3 and TiCN with size 45–55 nm

where less heating is required to avoid deformation. The development of the new method for modification of the liquid phase without remelting and through direct injection of the nanodispersed particles into the low-temperature zone of the weld pool will help to expand the nomenclature of composite materials and to enhance the wear resistance of some machine parts and elements. This innovative technology has been implemented to modify the surface layers of low-carbon steel pieces with Al_2O_3 and TiCN nanoparticles (45–55) nm (Fig. 1), as samples for microstructure, microhardness, and wear resistance testing are elaborated.

EXPERIMENTAL

Technology for preparation of overlaid samples. The material used for experimental weld overlay is low carbon structural steel S235JR (BSS EN 10025–2:2004) with chemical content shown in Table 1. The plates for weld overlay are cut out and the uneven edges are trimmed using abrasive disc. The dimensions of the plates and the scheme of weld overlay are shown in Fig. 2. The samples for weld overlay shall be cleaned to shine of rust, oil and dirt using sandpaper. If necessary, the surface can be flat-grinded. After cleaning the plates are fixed to the table for welding and continuous arc length with preset length ($L_a = 2$ mm) is provided.

Developed is a new method for nanomodification of the liquid phase through direct injection of the modifier into the weld pool. The optimum modes for remelt-

Table 1. Chemical content of S235JR steel

C (%)	Mn (%)	Si (%)	Cr (%)
0.1 – 0.15	1.6 – 1.8	0.4 – 0.8	0.2 – 0.4

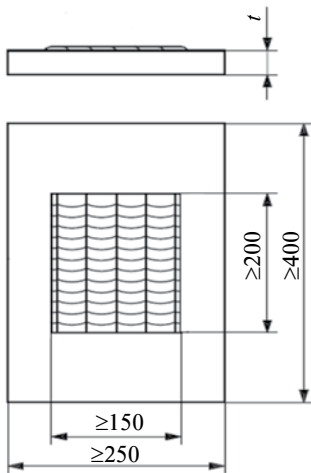


Fig. 2. Sample for weld overlay

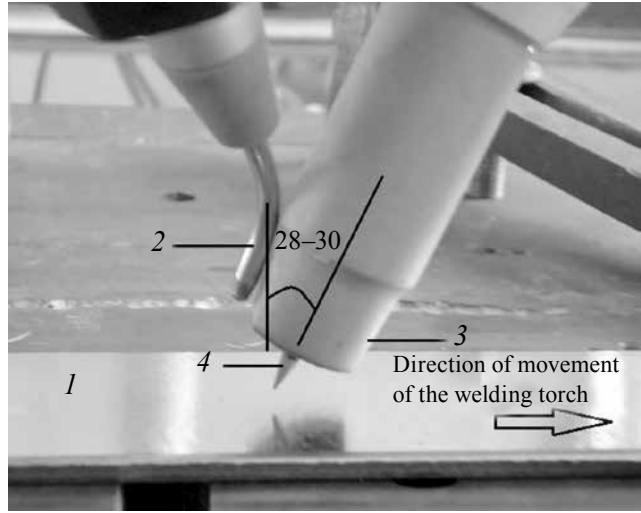
ing of strips of the surface of the test plates using the methods TIG/ITIG are determined in advance. The nanomodifier is fed through a special device with injector developed at angle $28\div 30^\circ$. The angle is determined during the experiments to find the manner for optimum feeding of the nanopowders. The powders are fed by the injector in the low temperature area of the weld pool after the tungsten electrode, opposite to the direction of movement of the welding torch (Fig. 3).

The methods used for remelting of the surface layer are TIG and ITIG.

Technologic parameters of TIG and ITIG weld overlay:

Fig. 3. Position of the torch and the injector during the process of weld overlay. The nanomodifier is fed in the low temperature area of the weld pool

I – grinded S235JR plate; 2 – injector for nanopowder; 3 – torch; 4 – tungsten electrode WL20



- current $I = 80$ A (for TIG);
- impulse current $I_{imp} = 120$ A, background current $I_b = 40$ A, average current $I_{av} = 80$ A (for ITIG);
- duration of the impulse and the pause 50%, i.e. $t_{imp} = t_p = 50\%$ (for ITIG);
- frequency of the impulse 4 Hz (for ITIG);
- arc voltage $U_a = 10.5 \div 11.5$ V;
- welding speed $V_{weld} = 2.5$ mm/s;
- flow rate of protective gas $Q_{gas} = 6 \div 7$ l/min Ar;
- electrode tungsten-lahntal, diameter $d_{el} = 2.4$ mm;
- electrode setback $L_{stb} = 6 \div 7$ mm;
- nozzle No 7, diameter $\varnothing 11$ mm;
- electrodeobliquity/drag angle $28 \div 30^\circ$.

The experimental surface modification of Al_2O_3 and TiCN with nanopowders at the above specified modes was carried out in accordance with two technological approaches for weld overlay: (1) conventional, through remelting of nanopowders pre-applied on the surface, and (2) new technology for direct injection of nanodispersed particles in the low temperature zone of the weld pool.

After the weld overlay, test samples with dimensions 15×15 mm (Fig. 4) for abrasion and wear-resistance testing were cut out through water jet cutting.

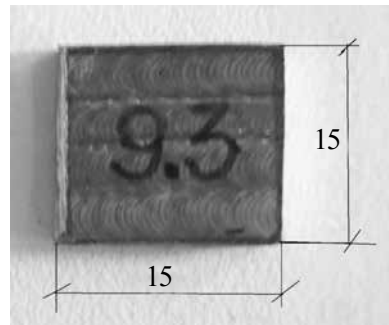


Fig. 4. Test sample for abrasion and wear resistance

Method and device for study of wear resistance. The method to study the characteristics of abrasion is developed by the authors herein and is based on the measurement of mass loss of samples for a definite path of abrasion at permanent conditions, e.g. load, speed of sliding, intensity of wear and wear resistance¹⁶.

The experimental part of the method involves the following steps:

– Elaboration of samples with dimensions 15×15 mm.

– Measurement of the initial mass m_0 using electron scale WPS 180/C/2 with accuracy of 0.1 mg. Prior to each measurement the scale is cleaned of mechanical and organic dirt and is dried with ethyl alcohol to prevent the electrostatic effect.

– The sample is attached to the holder of the loading head of the tribotester; then a certain normal load P is applied and a certain path L of friction is travelled.

– The mass m_i of the sample is measured after abrasion.

– The characteristics of mass wear are calculated:

Mass loss m (mg) is the mass destroyed during abrasion while the sample travels along the path of friction L , i.e.:

$$m = m_0 - m_i. \tag{1}$$

Mass wear rate γ (mg/min) is the mass destroyed per unit time during time for abrasion t :

$$\gamma = \frac{m}{t}. \tag{2}$$

Intensity of linear wear ($\mu\text{m}/\text{m}$) is the variation of the height of the sample, i.e. the linear wear h (μm) (Fig. 5) after travelling a certain path of friction L :

$$i = \frac{m}{\rho A_a L} = \frac{h}{L} \tag{3}$$

where ρ is the density of the surface layer, A_a – the nominal (geometric) area of contact.

Linear wear resistance I ($\text{m}/\mu\text{m}$) is reciprocal of the linear mass wear i :

$$I = \frac{1}{i} = \frac{\rho A_a L}{m}. \tag{4}$$

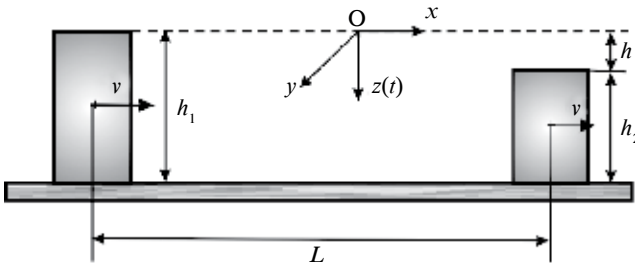
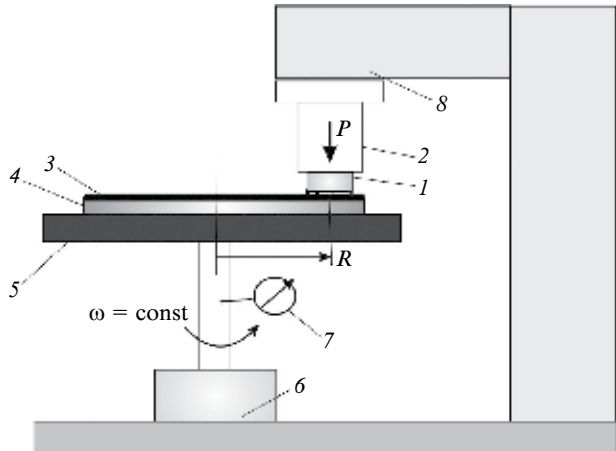


Fig. 5. Linear wear of the sample after travelling a certain path of friction

Fig. 6. Schematic view of tribotester ‘Finger-disc’ for testing of wear with fixed sample and rotating abrasive disc



The wear resistance I is indicative for the path of friction which the sample shall travel in order to reduce the depth of its surface layer with $1 \mu\text{m}$.

The comparison for wear resistance between different parts shall be performed under the same test conditions.

The abrasion wear in conditions of dry friction is examined using the tribotester in Fig. 6 operating upon kinematic scheme ‘finger-disc’^{17,18}.

The examined coated sample I (finger) is firmly attached in the groove of the holder 2 of the loading head 8 in a manner that the coated surface contacted with the abrasive surface of the horizontal disc 4 . The disc is driven by electric motor 6 and revolves around its vertical axis with angular velocity $\omega = \text{const}$.

The normal load P is applied in the centre of gravity of the area of contact between the sample and the abrasive surface and is weighed via lever system position within the loading head. The path of friction is defined by the number of revolutions of the cyclometer 7 and is calculated using the formula $L = 2\pi RN$, where R is the distance between the axis of revolution of the disc 4 and the axis of the sample I , and N is the number of cycles of abrasion. The nominal contact pressure is calculated using the formula $p_a = P/A_a$.

The abrasion surface 3 is impregnated corundum (E) with hardness 9.0 on the Moos scale that meets the requirement for at least 60% higher hardness than that of the tested material.

The conditions of the experiment are presented in Table 2.

Table 2. Parameters of the testing for wear resistance

Normal loading	$P = 4.53 \text{ N}$
Nominal contact surface	$A_a = 225 \cdot 10^{-6} \text{ m}^2$
Nominal contact pressure	$p_a = 2.01 \text{ N/cm}^2$
Average speed of sliding	$V = 13.1 \text{ cm/s}$
Abrasive surface	corundum P 120

RESULTS AND DISCUSSION

Study of wear resistance. Table 3 exhibits the results obtained for the characteristics of abrasion and wear resistance of all examined samples for different paths of friction. The methods used for remelting of the surface layer are TIG and ITIG. The results for abrasion and wear resistance of remelted strips of sample 1 using the two methods are averaged due to overlapping data. In samples 7 and 8 the nanomodification with TiCN is carried out through remelting of a pre-applied layer.

Table 3. Characteristics of abrasion and wear resistance of nanomodified samples and the reference sample

Number of cycles N	200	400	600	1000
Time t (min)	0.96	1.92	2.88	4.8
Sliding distance L (m)	46.4	92.8	139.2	232
Sample No 1: reference sample – averaged values from strips remelted using TIG and ITIG without nanomodification				
Mass loss m (mg)	46.8	85.7	109.8	138.2
Wear rate γ (mg/min)	48.75	44.6	38.2	28.8
Wear intensity i ($\mu\text{m}/\text{m}$)	5.75	5.3	4.5	3.4
Wear resistance I ($\text{m}/\mu\text{m}$)	0.17	0.19	0.22	0.29
Sample No 3: TIG + TiCN nanopowder; direct injection in the weldpool				
Mass loss m (mg)	29.7	56.1	79.5	102.7
Wear rate γ (mg/min)	31	29.2	27.6	21.4
Intensity i ($\mu\text{m}/\text{m}$)	3.65	3.4	3.25	2.52
Wear resistance I ($\text{m}/\mu\text{m}$)	0.27	0.29	0.31	0.4
Sample No 4: ITIG + TiCN nanopowder; direct injection in the weldpool				
Mass loss m (mg)	34.1	66.2	87.6	101.3
Wear rate γ (mg/min)	35.5	34.5	30.4	21.1
Intensity i ($\mu\text{m}/\text{m}$)	4.19	4.06	3.6	2.6
Wear resistance I ($\text{m}/\mu\text{m}$)	0.24	0.25	0.28	0.38
Sample No 5: TIG+ Al_2O_3 nanopowder; direct injection in the weldpool				
Mass loss m (mg)	50.3	78.8	97.2	117.1
Wear rate γ (mg/min)	52.4	41.1	33.75	24.4
Intensity i ($\mu\text{m}/\text{m}$)	6.2	4.85	4.14	2.87
Wear resistance I ($\text{m}/\mu\text{m}$)	0.16	0.21	0.24	0.35
Sample No 6: ITIG + Al_2O_3 nanopowder; direct injection in the weldpool				
Mass loss m (mg)	39.3	73.1	94.3	121.6
Wear rate γ (mg/min)	41	38.1	32.4	25.3
Intensity i ($\mu\text{m}/\text{m}$)	4.8	4.5	4	3.1
Wear resistance I ($\text{m}/\mu\text{m}$)	0.21	0.23	0.25	0.32
Sample No 7: TIG + TiCN nanopowder; remelting of pre-applied layer				
Mass loss m (mg)	44.7	68	96	126.9
Wear rate γ (mg/min)	46.6	35.4	33.3	26.4
Intensity i ($\mu\text{m}/\text{m}$)	4.5	4.15	3.9	3.1
Wear resistance I ($\text{m}/\mu\text{m}$)	0.18	0.24	0.3	0.3
Sample No 8: ITIG+ TiCN nanopowder; remelting of pre-applied layer				
Mass loss m (mg)	37.2	66.4	98.7	124.3
Wear rate γ (mg/min)	38.75	34.6	34.3	26
Intensity i ($\mu\text{m}/\text{m}$)	4.57	4.1	4	3.1
Wear resistance I ($\text{m}/\mu\text{m}$)	0.22	0.24	0.25	0.31

Fig. 7. Dependence of wear rate on the path of friction

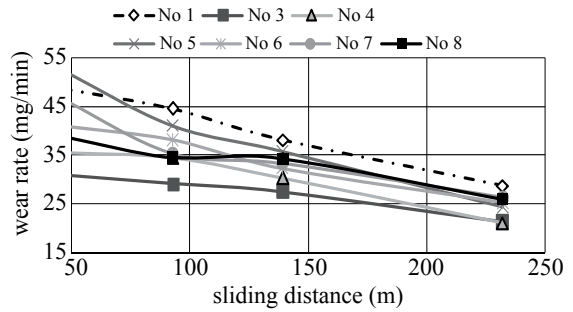
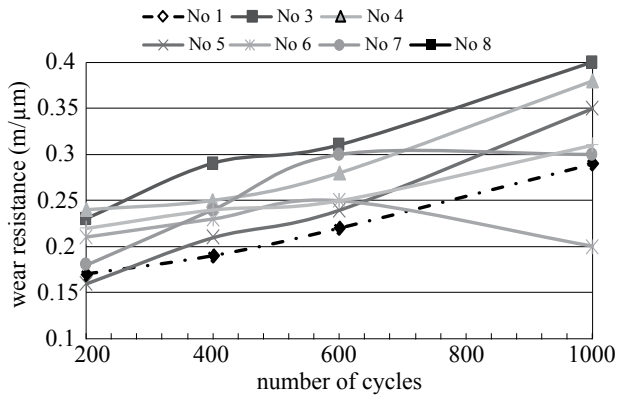


Fig. 8. Dependence of wear resistance on the number of cycles of friction



The dependence of the rate of wear on the path of friction and the dependence of wear resistance on the number of cycles of friction for all examined specimens are presented graphically in Figs 7 and 8, respectively.

The variation of the rate of wear is linear and decreases with the increase of the road friction for almost all samples. A certain nonlinearity is observed in sample No 7 up to path of friction $L = 92.8$ m.

The examination for wear resistance of the nanomodified samples is made at the same number of cycles of friction $N = 1000$.

It is obvious from the diagram of wear resistance in Fig. 9 that all samples examined have higher wear resistance in stationary mode than sample No 1 (without nanomodification).

Sample No 3 obtained using TIG method with injection of TiCN in the low-temperature area of the weld pool has the highest wear resistance with value about 1.4 times higher than that of the reference sample.

The lowest wear resistance is observed in the coatings of sample No 7 and sample No 8 nanomodified with remelting of pre-applied TiCN powder upon TIG and ITIG methods, respectively.

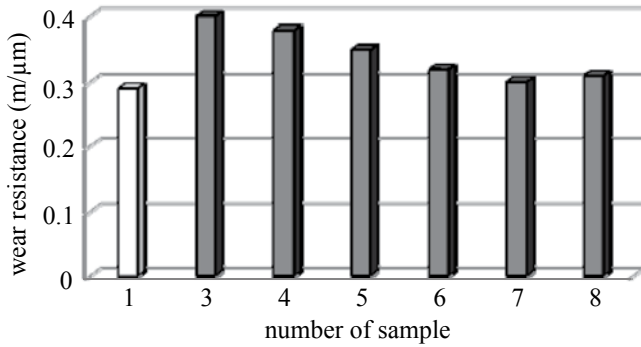


Fig. 9. Wear resistance of the samples at cycles of friction $N = 1000$

Study of microstructure. The metallographic specimens are made out of the overlaid samples following the methodology developed. The microstructure is observed using metallographic microscope with magnification $\times 100$.

In Figs 10 and 11 are shown microstructures of strips remelted upon TIG and ITIG methods, respectively. In Figs 12 and 13 are shown microstructures of strips remelted upon TIG and ITIG, respectively, with direct injection of TiCN nanopowder. The microstructure observed is bainitic (Fig. 12), as the finest bainite is obtained using the TIG method with direct injection of TiCN.



Fig. 10. Microstructure of remelted strip, TIG, $\times 100$



Fig. 11. Microstructure of remelted strip, ITIG, $\times 100$

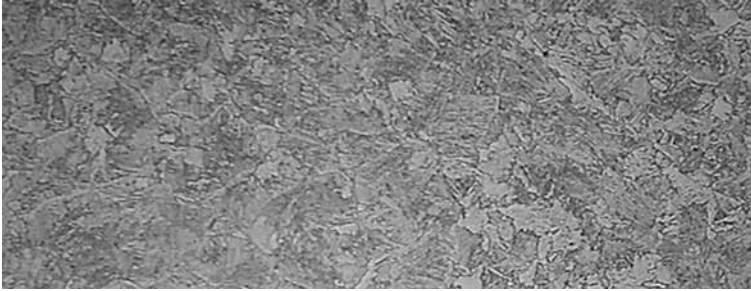


Fig. 12. Microstructure of remelted strip, TIG+TiCN with injection of nanoparticles, ×100

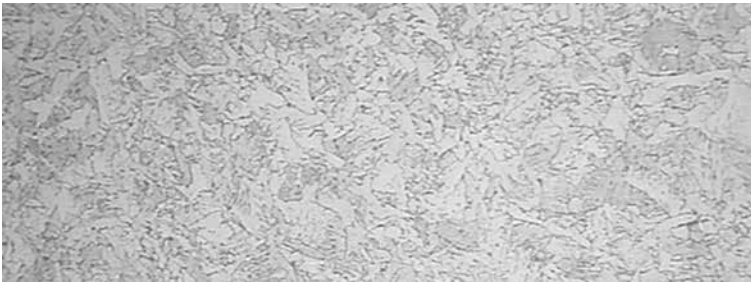


Fig. 13. Microstructure of remelted strip, ITIG+TiCN with injection of nanoparticles, ×100

Measurement of Vickers microhardness. The measurement of microhardness HV 0.1 is made in selected areas of the overlaid metal and the base metal. The highest microhardness is achieved using TIG method with modification with TiCN introduced through injection into the low-temperature zone of the weld pool. The graph shown in Fig. 14 visualises the results for the variation of microhardness

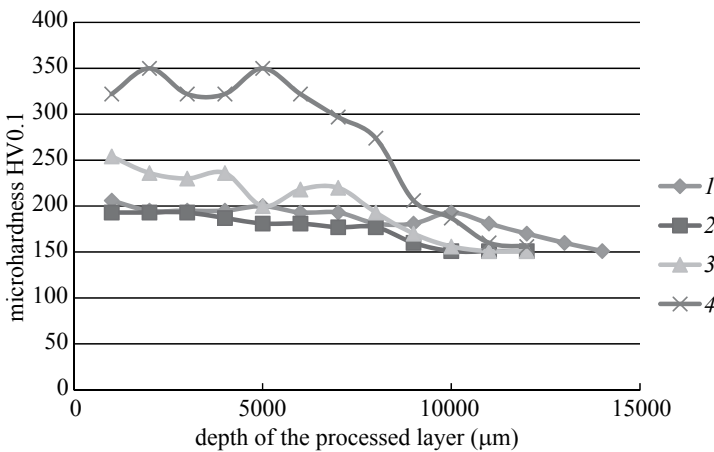


Fig. 14. Variation of microhardness along the depth of the processed layer of test samples remelted using methods TIG (curve 1) and ITIG (curve 2) without modification, and samples with directly injected TiCN nanopowder using methods ITIG (curve 3) and TIG (curve 4)

along the depth of the processed layer of the test specimens remelted using methods 1 (TIG), 2 (ITIG) without nanomodification and specimens modified through direct injection of TiCN nanopowder using methods 3 (ITIG) and 4 (TIG).

CONCLUSIONS

- Developed is innovative technology for introduction of nanosized particles through direct injection in the low-temperature zone of the weld pool behind the weld arc using TIG and ITIG methods.

- The surface layers of test samples are modified according to technological modes specified in advance with introduction of Al_2O_3 and TiCN nanopowders by two methods: (1) conventional technology consisting in remelting of pre-applied nanomaterial, and (2) the new technology developed.

- Comparative study is conducted for wear resistance according to the method of accelerated wear from abrasive surface.

- The lower values of microhardness and wear resistance established in case of nanomodification upon ITIG method compared to those obtained upon TIG method are explained with the typical powerful current pulses in the case of ITIG that probably throw a part of the nanomodifier out of the melting zone and increase excessively the temperature in the zone of injection.

- The maximum wear resistance is achieved in specimen 3 (Table 3), whose surface is nanomodified with TiCN upon TIG method through direct injection of the nanomodifier in the low-temperature zone of the weld pool. The increase of wear resistance found is 27.5% compared to the reference specimen.

- The high value for wear resistance of specimen 3 (Table 3) can be explained with the fine-grain structure (Fig. 12) resulting from nanomodification and the properly selected technology of introduction of the nanomodifier. The same specimen exhibits the highest values of microhardness measured in depth.

ACKNOWLEDGEMENTS

This study is associated with the implementation of tasks on the subject of the project ‘Development of technology for arcweld overlay of wear resistant layers using nanomaterials’ financed by the National Innovation Fund – Sixth Session 2012 ID No IF-00-06-12.

REFERENCES

1. A. ARTEMEV, G. N. SOKOLOV, V. I. LYSAK: Effect of Microparticles of Titanium Diboride and Nanoparticles of Titanium Carbonitride on the Structure and Properties of Deposited Metal. *Metal Science and Heat Treatment*, **53** (11–12), (2012).

2. R. JAMAATI, M. R. TOROGHINEJAD, H. EDRIS: Effect of SiC Nanoparticles on Bond Strength of Cold Roll Bonded IF Steel. *Journal of Materials Engineering and Performance*, **22** (11), 3348 (2013).
3. YONG YANG, JIELAN, XIAOCHUN LI: Study on Bulk Aluminum Matrix nano-composite Fabricated by Ultrasonic Dispersion of Nano-sized SiC Particles in Molten Aluminum Alloy. *Materials Science and Engineering A*, **380**, 378 (2004).
4. A. S. TROSHKOV: Modification of the Structure of the Overlaid Metal by Means of Tungsten Nanodispersed Carbides. *Polzunovsky Almanac*, (2), 111 (2009) (in Russian).
5. V. O. DROZDOV, A. G. MALIKOV et al.: Experimental Study of Laser Welding of Metals Using Nanopowder Additives. Report at the V All-Russia Conference for Interaction Between Highly-concentrated Energy Flows and Materials in the Advanced Technologies in the Medical Sciences. Novosibirsk, March 26–29, 2013, 97–101 (in Russian).
6. P. TASHEV, T. PETROV, Y. LUKARSKI, G. STEFANOV: Technologies for Interduction of Nanosized Particles in the Weld During Processes of Weld Overlay. *Engineering Sciences*, **L** (3), 82 (2013) (in Bulgarian).
7. A. N. CHEREPANOV et al.: On the Implementation of Nanopowders of Refractory Compounds in Welding and Processing of Metals and Alloys. *Heavy Engineering*, (4/2), 25 (2008) (in Russian).
8. M. FATTAHI, N. NABHANI, M. R. VAEZI, E. RAHIMI: Improvement of Impact Toughness of AWS E6010 Weld Metal by Adding TiO₂ Nanoparticles to the Electrode Coating. *Materials Science and Engineering A*, **528**, 8031 (2011).
9. PANIAGUA-MERCADO, ANA MA., V. M. LOPEZ-HIRATA, H. J. DORANTES-ROSALES et al.: Effect of TiO₂-containing Fluxes on the Mechanical Properties and Microstructure in Submerged-arc Weld Steels. *Materials Characterization*, **60**, 36 (2009).
10. B. BEIDOKHTI, A. H. KOUKABI, A. DOLATI: Effect of Titanium Addition on the Microstructure and Inclusion Formation in Submerged Arc Welded HSLA Pipeline Steel. *Journal of Materials Processing Technology*, **209**, 4027 (2009).
11. P. TASHEV, M. KANDEVA, P. PETROV: An Investigation on the Wear Properties of Carbon Steel Coated with Nanoparticles Using Electron Beam Technique. *J Balk Tribol Assoc*, **20** (2), 227 (2014).
12. C. CUIXIN, P. HUIFEN, L. RAN et al.: Research on Inclusions in Low Alloy Steel Welds with Nano Alumina Addition. *Journal of Computational and Theoretical Nanoscience*, **9** (9), 1533 (2012).
13. M. TONGOV, T. SIMEONOVA: A Study on the Formation of Layers Obtained Through Highly-Concentrated Energy Sources. International Scientific Conference MTF'2012, November 18–20, 2012, TU-Sofia (in Bulgarian).
14. P. PETROV: Surface Modification of Aluminium Alloys Using Hybrid Treatment Techniques. *Journal of Physics: Conference Series*, 356 (2012).
15. St. HRISTOV, T. YAMBOLIEV, D. MADZHOV, P. DASKALOV, Iv. PANOV: Manual for Laboratory Experiments on the Technology of Machine Building Materials. Plovdiv, 1992 (in Bulgarian).
16. V. PETKOV, P. TASHEV, N. GIDIKOVA, M. KANDEVA, R. VALOV: Wear Resistant Chromium Coating with Diamond Nanoparticles upon an Arc Deposited Layer. *J Balk Tribol Assoc*, **20** (1), 134 (2015).
17. M. KANDEVA, B. IVANOVA: Abrasive Wear and Wear-Resistance of High Strength Cast Iron Containing Sn Microalloy. *J Balk Tribol Assoc*, **19** (4), 559 (2013).
18. I. PEICHEV, M. KANDEVA, E. ASSENOVA, V. POJIDAEVA: About the Deposition of Super-alloys by Means of Supersonic HVOF Process. *J Balk Tribol Assoc*, **17** (3), 380 (2011).

Received 5 August 2015
Revised 19 October 2015